JCB Journal of Cell Biology

REPORT

Centrobin is essential for C-tubule assembly and flagellum development in *Drosophila melanogaster* spermatogenesis

Jose Reina[1*], Marco Gottardo[2*], Maria G. Riparbelli[2], Salud Llamazares[1], Giuliano Callaini[2], and Cayetano Gonzalez[1,3]

Centrobin homologues identified in different species localize on daughter centrioles. In *Drosophila melanogaster* sensory neurons, Centrobin (referred to as CNB in *Drosophila*) inhibits basal body function. These data open the question of CNB's role in spermatocytes, where daughter and mother centrioles become basal bodies. In this study, we report that in these cells, CNB localizes equally to mother and daughter centrioles and is essential for C-tubules to attain the right position and remain attached to B-tubules as well as for centrioles to grow in length. CNB appears to be dispensable for meiosis, but flagellum development is severely compromised in *Cnb* mutant males. Remarkably, three N-terminal POLO phosphorylation sites that are critical for CNB function in neuroblasts are dispensable for spermatogenesis. Our results underpin the multifunctional nature of CNB that plays different roles in different cell types in *Drosophila*, and they identify CNB as an essential component for C-tubule assembly and flagellum development in *Drosophila* spermatogenesis.

Introduction

Centrobin was initially identified in humans through a yeast two-hybrid screen for proteins that interact with the tumor suppressor BRCA2 (Zou et al., 2005). Like human Centrobin (referred to as CNTROB in humans), its homologues in other species are components of daughter centrioles in different cell types (Zou et al., 2005; Januschke et al., 2011, 2013; Gottardo et al., 2015). In mammals, CNTROB has been reported to be required for centriole duplication and elongation as well as for microtubule nucleation and stability through its binding to tubulin and its effect in stabilizing centrosomal P4.1-associated protein (CPAP; Jeong et al., 2007; Jeffery et al., 2010, 2013; Gudi et al., 2011, 2014, 2015; Shin et al., 2015).

Drosophila melanogaster Centrobin (referred to as CNB in *Drosophila*) is a key determinant of mother/daughter centriole functional asymmetry in larval neuroblasts and type I sensory neurons. In neuroblasts, CNB functions as a positive regulator of microtubule organizing center (MTOC) activity during interphase: its depletion impedes daughter centrioles to assemble an MTOC, whereas mother centrioles carrying ectopic CNB become active MTOCs (Januschke et al., 2013). This activity is dependent on CNB phosphorylation by PLK1/POLO on three conserved sites (Januschke et al., 2013) and involves the function of pericentrin-like protein (PLP; Lerit and Rusan, 2013) and BLD10/CEP135 (Singh et al., 2014). In *Drosophila* type I sensory neurons, CNB functions as a negative regulator of ciliogenesis: CNB depletion enables daughter centrioles as functional basal bodies that template ectopic cilia, and mother centrioles modified to carry CNB cannot function as basal bodies (Gottardo et al., 2015).

The function of a daughter centriole protein like CNB as a negative regulator of ciliogenesis opens the question of CNB's role in *Drosophila* primary spermatocytes where after centrosome duplication all four centrioles, mothers and daughters alike become basal bodies that assemble axoneme-based cilium-like structures, which are the precursors of sperm flagella (Tates, 1971; Riparbelli et al., 2012, 2013; Gottardo et al., 2013). To investigate this issue, we have studied CNB localization and function in spermatogenesis.

Results and discussion

CNB localizes equally to mother and daughter centrioles in *Drosophila* primary spermatocytes

As in other cell types in *Drosophila* and other species, CNB localization in spermatogonial cells was asymmetric, restricted to only one of the two centrioles that were labeled with anti-SAS4 antibodies (Fig. 1 A, red and green, respectively; $n = 86$ cells from

[1]Institute for Research in Biomedicine (IRB Barcelona), The Barcelona Institute of Science and Technology, Barcelona, Spain; [2]Department of Life Sciences, University of Siena, Siena, Italy; [3]Institució Catalana de Recerca i Estudis Avançats, Barcelona, Spain.

*J. Reina and M. Gottardo contributed equally to this paper; Correspondence to Cayetano Gonzalez: gonzalez@irbbarcelona.org; M. Gottardo's present address is Center for Molecular Medicine, University of Cologne, Cologne, Germany.

https://doi.org/10.1083/jcb.201801032

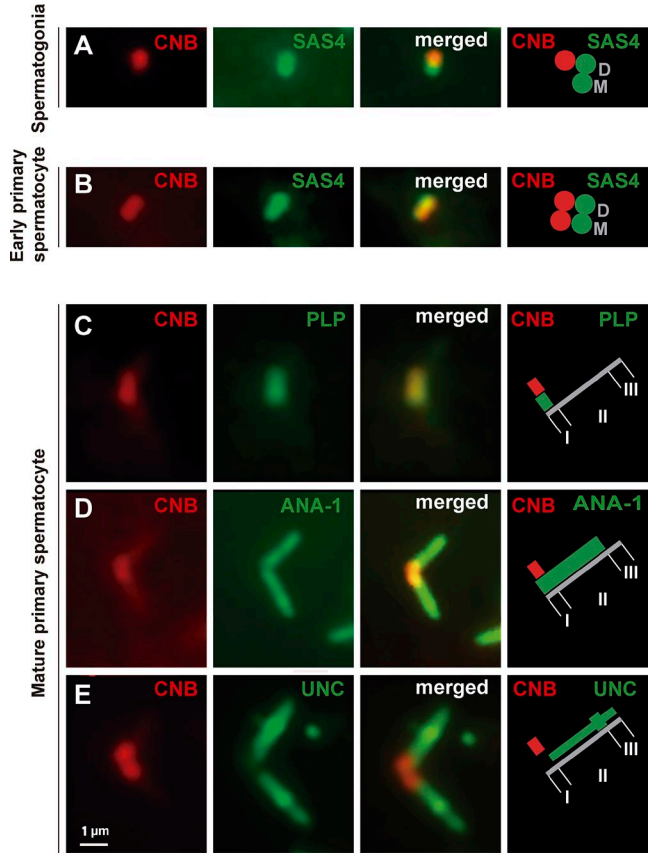

Figure 1. **CNB localizes equally in mother and daughter centrioles in primary spermatocytes. (A and B)** CNB (red) localized to only one of the of the two SAS4-positive (green) centrioles, presumably the daughter (D in the cartoon), in spermatogonia (A; *n* = 86 cells from 25 cysts), but it colocalized with the two centrioles—mother (M in the cartoon) and daughter—in early primary spermatocytes (B; *n* = 163 cells from 15 cysts). **(C–E)** CNB signal (red) was equal in the two basal bodies of a pair. The region of highest concentration of CNB (region I) overlapped with PLP (C) on the proximal end of the ANA1 domain (D), where UNC concentration was lowest (E). Weak CNB and PLP signal could also be detected all along the basal body (C–E; region II; *n* = 247 cells from 98 cysts).

25 spermatogonial cysts). However, after the last (fourth) round of spermatogonial mitosis, the resulting early primary spermatocytes presented CNB equally distributed on the two centrioles of each pair (Fig. 1 B; *n* = 163 cells from 15 cysts).

After centrosome duplication, all four centrioles of each spermatocyte grow significantly in length, migrate to the cell surface, and become basal bodies that template a short axoneme that forms a protrusion covered by the cell membrane (Tates, 1971; Fritz-Niggli and Suda, 1972). Recent studies refer to this protrusion as the cilium-like region (CLR; Gottardo et al., 2013) or the ciliary cap (Vieillard et al., 2016).

To determine CNB localization in the basal body–CLR complex, we immunostained CNB together with PLP, ANA1, and UNC. PLP signal was strongest on the proximal end of the basal body (Fig. 1 C, region I; Fu and Glover, 2012; Galletta et al., 2014). ANA1 labelled the entire length of the basal body (Fig. 1 D, regions I and II; Blachon et al., 2009; Riparbelli et al., 2012, 2013; Basiri et al., 2014). UNC overlapped with ANA1 except on the PLP-positive proximal end, was strongest at the transition zone, and extended further distally into the axoneme (Fig. 1 E, regions II and III; Baker et al., 2004; Ma and Jarman, 2011; Riparbelli et al., 2012). We found that CNB signal was equal in all basal bodies (*n* = 247 cells from 98 cysts); most concentrated on the proximal end of the ANA1 domain, largely overlapping with PLP. Like PLP, a very weak CNB signal could also be detected all along the basal body (Fig. 1, C–E, region II). These observations reveal some remarkable differences regarding CNB localization, which in turn suggest important functional differences as far as ciliogenesis is concerned between early spermatocytes and sensory neurons in *Drosophila*.

CNB is required in primary spermatocytes for basal bodies to achieve normal length and for the proper assembly of the C-tubule

To determine whether CNB has a function in the basal body–CLR complex, we examined trans-heterozygous *PBac(RB)Cnb[e00267]/Df(3L)ED4284* (henceforth referred to as *Cnb* mutant) spermatocytes. We found that the length of YFP-Asterless (ASL) signal (a proxy for centriole length) was significantly shorter ($P < 0.001$) in *Cnb* mutant (0.97 ± 0.28 µm) than in WT males (1.55 ± 0.11 µm; Fig. 2, A and C, gray bars). Longitudinal EM sections from centriole pairs in which both mother and daughter were cut along their entire length confirmed this observation (Fig. 2, B, D, and E) and revealed that daughter basal bodies were shorter than their mothers in *Cnb* mutant spermatocytes (0.62 ± 0.07 µm and 0.78 ± 0.04 µm, respectively; *n* = 5 centriole pairs; Fig. 2 E and Table S2). This was not the case in WT spermatocytes, where as previously reported (Riparbelli et al., 2012), we found that mother and daughter basal bodies were of equal length (1.02 ± 0.04 µm and 1.00 ± 0.05 µm, respectively; *n* = 5 centriole pairs; Fig. 2 E and Table S2). EM sections also revealed that 10 out of 16 mutant axonemes sectioned longitudinally were irregularly

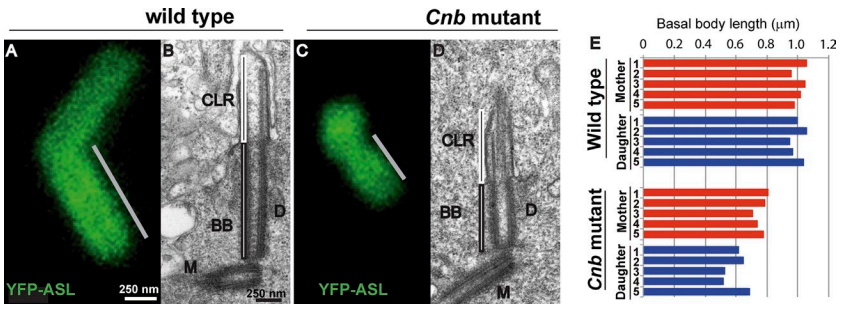

Figure 2. **Basal bodies are shorter in *Cnb* mutants than in WT spermatocytes. (A–D)** Basal bodies (BBs) revealed by YFP-ASL fluorescence (A and C, green) and basal body–CLR complexes observed in EM longitudinal sections (B and D) from WT (A and B) and *Cnb* mutant (C and D) mature spermatocytes. M and D indicate basal bodies derived from mother and daughter centrioles, respectively. Gray bars show the length of the YFP-ASL signal. **(E)** Basal body length measured from EM longitudinal sections of five mother (red)/daughter (blue) pairs (numbered) from WT and *Cnb* mutant mature spermatocytes.

shaped and had abnormal axonemes with doublets that were aberrantly interrupted halfway through the CLR (Fig. 2 D).

We then examined the ultrastructural details revealed by transversal EM sections. As reported previously (Gottardo et al., 2015), unlike basal bodies in sensory neurons that are made of doublets, basal bodies in WT spermatocytes are made of triplets (Fig. 3, A and A′). At the transition zone, the outermost tubule (C-tubule) progressively lost protofilaments (Fig. 3, B and B′), hence becoming an open longitudinal sheet that extended beyond the transition zone along the axoneme (Fig. 3, C and C′, red arrow). At the point where C-tubule remnants and B-tubules intersect, short radial projections could be observed (Fig. 3, C and C′, blue arrow; Riparbelli et al., 2012).

In addition to this basic layout of triplets, doublets, and open sheaths, about half of basal body–CLR complexes in *Drosophila* WT spermatocytes present a luminal singlet microtubule independently of the Z position of the cross-section (Tates, 1971; Carvalho-Santos et al., 2012; Riparbelli et al., 2012). The presence of this luminal singlet is as erratic in *Cnb* mutant as it is in WT males and does not represent a *Cnb* mutant phenotype.

We serially sectioned 11 basal body–CLR complexes from two *Cnb* mutant males. In all 11 samples, C-tubules were either misplaced outwards, away from the nearly straight line defined by the A/B doublet (Fig. 3, D and D′, blue), or lost, leaving only duplets behind (Fig. 3, D, D′, G, and G′, green; Table S1). These abnormalities extended distally along the axoneme, where C-tubule–derived longitudinal sheets were often lacking in *Cnb* mutant spermatocytes (Fig. 3, E–F′ and H–I′, red arrow). The short radial projections observed in WT axonemes (Fig. 3, C and C′, blue arrow) also appeared to be lacking in *Cnb* mutant CLRs (Fig. 3, F, F′, I, and I′, blue arrow), but this observation must be interpreted with caution because of the technical difficulties of detecting such small structures that are located in regions of electron-dense material.

These observations reveal that CNB is required in *Drosophila* spermatocytes for centrioles to properly position and stabilize C-tubules, grow in length up to full-sized basal bodies, and template normal axonemes. Our results identify CNB as one of the very few proteins known so far to be required for C-tubule assembly, including Δ-tubulin in *Paramecium tetraurelia* (Garreau de Loubresse et al., 2001) and *Chlamydomonas reinhardtii* (Dutcher and Trabuco, 1998) along with *UNC* and *SAS4* in *Drosophila* (Gottardo et al., 2013; Zheng et al., 2016). Notably, as in *Cnb* mutant spermatocytes, basal bodies are also shorter than normal in *Sas4*^{F112A} and *Unc* mutant spermatocytes (Gottardo et al., 2013; Zheng et al., 2016), hence suggesting that short centrioles and lacking or mispositioned C-tubules may be causally linked.

Drosophila SAS4 and its human homologue CPAP are closely functionally related to the corresponding Centrobin homologues CNB/CNTRB. Mutants in the N-terminal helical motif of the PN2-3 domain of CPAP and SAS4 cause overelongation of newly formed centriolar/ciliary microtubules, and so does CNTRB overexpression by stabilizing and driving the centriolar localization of CPAP (Gudi et al., 2011, 2014, 2015). Moreover, the mutants in PN2-3 domain of CPAP referred to above result in biciliated cells, and so does *Cnb* loss of function in *Drosophila* sensory neurons.

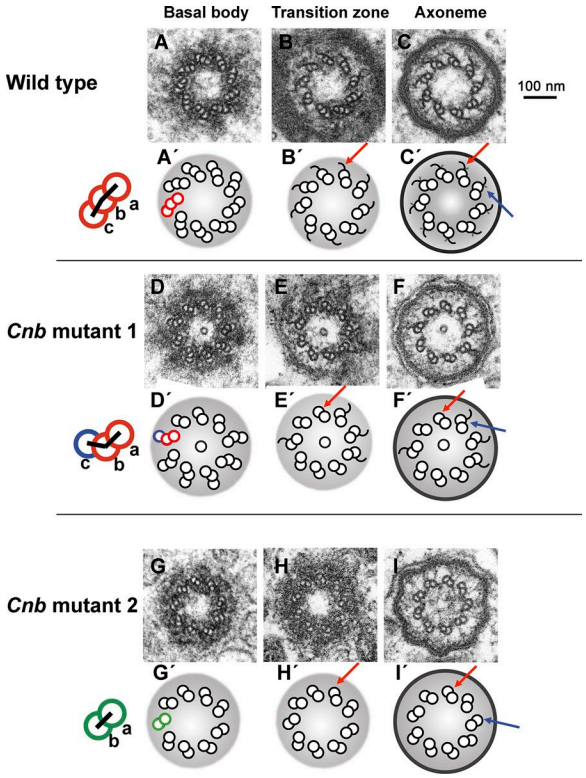

Figure 3. **C-tubules are mispositioned or lacking in the basal bodies in *Cnb* mutant spermatocytes. (A–C′)** Serial sections through a basal body (A and A′), transition zone (B and B′), and axoneme (C and C′) from a WT primary spermatocyte. Basal bodies presented triplets composed of A-, B-, and C-tubules arranged along a nearly straight line (cartoon, red). At the transition zone, the outermost tubule (C-tubule) progressively lost protofilaments and became an open sheet (B and B′, red arrow). C-tubule remnants extended along the axoneme (C and C′, red arrow). Short radial projections could be observed in the axoneme at the point where C-tubule remnants and B-tubules intersected (C and C′, blue arrow). **(D–I′)** Serial sections through basal bodies, transition zones, and axonemes from two *Cnb* mutant primary spermatocytes (*Cnb* mutants 1 and 2). In all 11 serially sectioned samples, C-tubules in *Cnb* mutant basal bodies were either mispositioned away (blue tubule) from the straight line defined by the A/B doublet (red tubules) or lacking leaving doublets behind (green). *Cnb* mutant transition zones often lacked C-tubule–derived longitudinal sheets (E, E′, H, and H′, red arrow) and so did mutant axonemes (F, F′, I, and I′, red arrows), which also lacked the short radial projections observed in WT axonemes (F, F′, I, and I′, blue arrows). Neither the WT cell shown in this figure (A–C′) nor Cnb mutant 2 (G–I′) presented a microtubule in the center of the lumen, but Cnb mutant 1 did (D–F′). The presence of this luminal singlet was as erratic in *Cnb* mutant as it was in WT males and does not represent a *Cnb* mutant phenotype.

In *Drosophila*, SAS4 and CNB coimmunoprecipitate from embryo extracts (Januschke et al., 2013). These data strongly suggest that the role of CNB on basal body length may be SAS4 dependent.

Elongating axonemes are abnormal in *Cnb* mutant males

The ultrastructural phenotypes that we have observed in basal body–CLR complexes in *Cnb* mutant spermatocytes persist through meiosis and are present in early postmeiotic cells (Fig. S1 A). However, we did not detect any observable defects in meiosis. *Cnb* mutant males assembled fairly normal meiotic spindles and generated normal cysts of postmeiotic onion-stage spermatids

that presented a uniform nuclear size (Fig. S1 B), which is a very sensitive readout of faithful meiotic chromosome segregation (González et al., 1989). These results strongly suggest that shortened centrioles and lacking C-tubules have no major observable consequences on meiosis progression.

However, soon after meiosis, when the basal body attaches to the nucleus and the axoneme starts to grow, pushing the old CLR caudally, *Cnb* mutant spermatids presented CLRs that were much longer than those from WT cells: 5.6 ± 1.4 µm (n = 7) and 1.5 ± 0.8 µm (n = 6), respectively (Fig. 4, A and B). Abnormally long CLRs have also been reported in *Unc* mutant early spermatids (Gottardo et al., 2013). In WT cells at this stage, CNB signal was strongest on the basal body proximal to UNC and was also detectable over the perinuclear plasm (Tates, 1971), a cap over the nuclear hemisphere where the basal body is engaged (Fig. S1 C).

Cnb mutant phenotypes were also conspicuous at later stages of elongation. Transversal sections through the tails of WT elongating spermatids showed two mitochondrial derivatives flanking the axoneme, which was almost completely surrounded by a double membrane (Fig. 4 C). Among the sample of 32 *Cnb* mutant elongating spermatids that we analyzed in detail (belonging to three cysts from two different males), we found a wide range of phenotypic variability (Fig. 4, D–G). Five presented a fairly WT 9 + 2 configuration, whereas the other 27 included cells that had no axoneme (n = 5; Fig. 4 D, NA) or axonemes with missing or highly disarrayed duplets and in which the surrounding membrane was widely open (n = 22; Fig. 4, E and F). Among the latter, six had some duplets that carried C remnants, and 16 did not. Interestingly, not all duplet-bound open sheaths observed in *Cnb* mutant cells were C remnants, such as for instance the one shown in Fig. 4 F that originated from an A-tubule and was oriented in the wrong direction. We also found four axonemes that presented one to three triplets with an attached open sheath (Fig. S2 A, arrows). No such structures have been reported in WT cells. The presence of a fraction of *Cnb* mutant spermatids with axonemes that presented C remnants suggests that a certain fraction of *Cnb* mutant primary spermatocytes retain C-tubules.

In addition to lacking and disarranged axonemes, *Cnb* mutant elongating spermatids also presented ectopic nuclei at sections where only tails were present in WT cysts (Fig. 4 G, Nu, and Fig. S2 B). Scattered nuclei have also been reported in other *Drosophila* mutants like *Unc* and *Sas4* (Baker et al., 2004; Riparbelli and Callaini, 2011). Head-to-tail attachment defects have been documented in the sperm of a rat CNTROB mutant strain (hd rats) that was male sterile (Liška et al., 2013).

Our results reveal that CNB depletion brings about a spectrum of mutant phenotypes at different stages of spermatogenesis that includes shorter centrioles, mispositioned or absent C-tubules, lack of C-tubule derivatives, abnormal or absent axonemes, and scattered nuclei along elongating spermatid bundles. We cannot discard that CNB may have independent functions accounting for each of these phenotypes. However, the apparent pleiotropic effect of CNB loss may simply reflect the downstream consequences of centrioles that are shorter than normal and present C-tubule defects.

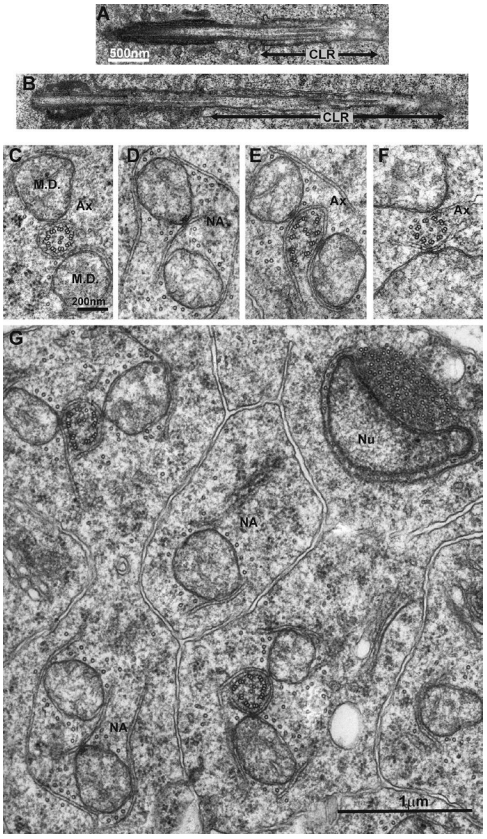

Figure 4. **Axonemes are often malformed or lost in *Cnb* mutant spermatids. (A and B)** Longitudinal sections through the basal body and axoneme (Ax) in WT (A) and *Cnb* mutant (B) early spermatids. The CLR (black line) was longer than normal in *Cnb* mutant spermatids (5.6 ± 1.4 µm, n = 7, and 1.5 ± 0.8 µm, n = 6, respectively). **(C)** Section through the tail of a WT elongating spermatid showing the axoneme that presented the typical 9 + 2 configuration flanked by two mitochondrial derivatives (M.D.s). **(D–F)** Sections through *Cnb* mutant elongating spermatid showing one without axoneme (no axoneme [N.A.]; D) and axonemes that presented duplets with and without C remnants (E and F). **(G)** General view revealing phenotypic variation among *Cnb* mutant spermatids of the same cyst including a cell that had no axoneme and presented a single mitochondrial derivative and the nucleus (Nu) of an ectopic spermatid head.

Amino acids T4, T9, and S82, which are critical for centriole asymmetry in *Drosophila* neuroblasts, are dispensable for CNB function in spermatogenesis

Expression of YFP-CNB^{WT}, a fusion protein between YFP and WT CNB, rescued all the phenotypes that we observed in *Cnb* mutant males. These included (A) the ultrastructural abnormalities, which affected premeiotic basal body–CLR complexes and postmeiotic axonemes (Fig. 5, A–D), (B) centriole (YFP-ASL) length (Fig. 5 I), which was rescued from 0.97 ± 0.28 µm (n = 27) in *Cnb* mutant males to 1.47 ± 0.16 µm (n = 20), very close to WT length (1.55 ± 0.11 µm, n = 21), and (C) fertility (Fig. 5 J), which was rescued to 81 ± 7, which is indistinguishable from WT levels (87 ± 4; offspring per male in single-pair mating tests; n = 15). These results confirm that all these phenotypes are indeed brought about by *Cnb* loss of function and are not caused by other unrelated mutations.

Remarkably, all these *Cnb* mutant traits were also rescued by the YFP-CNB$^{T4A\text{-}T9A\text{-}S82A}$ transgene (Januschke et al., 2013).

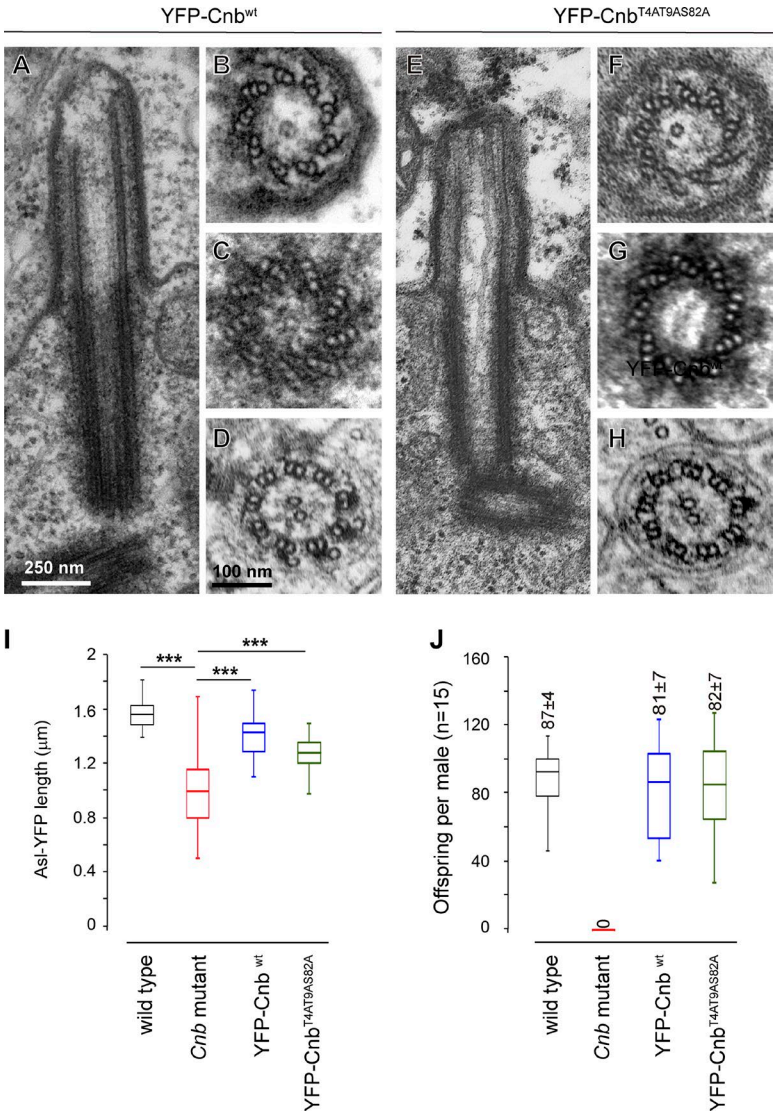

Figure 5. **CNB^{WT} and CNB$^{T4A\text{-}T9A\text{-}S82A}$ are equally capable of rescuing CNB mutant traits in spermatogenesis. (A–H)** EM longitudinal sections through basal body–CLR complexes (A and E) and transversal sections through premeiotic axonemes (B and F) and basal bodies (C and G) as well as postmeiotic axonemes (D and H) from *Cnb* mutant males expressing the YFP-CNB^{WT} (A–D; nine longitudinal sections through CLRs, five and 11 cross sections through basal bodies and CLRs, respectively, and 67 cross sections through elongating spermatids from six cysts) or the YFP-CNB$^{T4A\text{-}T9A\text{-}S82A}$ construct (E–H; seven longitudinal sections through CLRs, six and 13 cross sections through basal bodies and CLRs, respectively, and 38 cross sections through elongating spermatids from four cysts). **(I)** Basal body length (YFP-ASL fluorescence) in WT (n = 21), *Cnb* mutant (n = 27), *Cnb* mutant expressing YFP-CNB^{WT} (n = 20), and *Cnb* mutant expressing YFP-CNB$^{T4A\text{-}T9A\text{-}S82A}$ males (n = 17). ***, P < 0.001 (ANOVA). **(J)** Fertility of WT, *Cnb* mutant, *Cnb* mutant expressing YFP-CNB^{WT}, and *Cnb* mutant expressing YFP-CNB$^{T4A\text{-}T9A\text{-}S82A}$ single males (n = 15). Error bars indicate SEM.

Basal bodies, CLRs, and spermatids recovered WT ultrastructure including properly positioned C-tubules and C-tubule remnants (Fig. 5, E–H); centriole (YFP-ASL) length was recovered to 1.26 ± 0.14 µm (n = 17); and, notably, the amount of offspring per male in single-pair mating experiments was also fully recovered to WT levels (82 ± 7; n = 15; Fig. 5 J).

YFP-CNB$^{T4A\text{-}T9A\text{-}S82A}$ carries a mutant version of CNB in which three consensus POLO phosphorylation sites have been substituted by alanine. In larval neuroblasts, YFP-CNB$^{T4A\text{-}T9A\text{-}S82A}$ retains specific daughter centriole binding, but unlike YFP-CNB^{WT}, it does not rescue the loss of PCM and microtubule aster during interphase caused by *Cnb* loss of function (Januschke et al., 2013). The efficient rescue of *Cnb* mutant traits in spermatogenesis by YFP-CNB$^{T4A\text{-}T9A\text{-}S82A}$ strongly suggests that CNB phosphorylation by POLO in these three critical sites is not necessary for CNB function during spermatogenesis, hence underpinning the diversity of cell type–specific molecular functions of CNB.

The different, and in some aspects opposite, roles of CNB in basal body structure and ciliogenesis in type I sensory neurons and spermiogenesis are remarkable. In neurons, CNB inhibits basal body function on the centriole to which it binds that in WT cells is only the daughter centriole (Gottardo et al., 2015). In primary spermatocytes, however, CNB localizes to both mother and daughter centrioles, which in these cells are equally able basal bodies, and acts as a positive regulator of ciliogenesis (Tates, 1971; Fritz-Niggli and Suda, 1972; Gottardo et al., 2013). One conspicuous difference between these two cell types is that basal bodies in spermatocytes contain C-tubules, whose assembly, positioning, and stability requires CNB. In vertebrates, where centrioles also have C-tubules, a recent study has found that in addition to its primary localization to daughter centrioles, CNTROB associates with mother centrioles at the onset of ciliogenesis, and CNTROB loss causes defective axonemal extension (Ogungbenro et al., 2018). These results suggest that the different effect that CNB depletion has on ciliogenesis in *Drosophila* neurons and spermatocytes may reflect the doublet versus triplet structure of the corresponding basal bodies.

Materials and methods

Fly stocks and husbandry

The following fly stocks were used in this study: PBac{RB}Cnb^{e00267} (Exelexis); Df(3L)ED4284 (Bloomington Drosophila Stock Center); pUbqYFP-ASL (Rebollo et al., 2007); ANA1-GFP (from T. Avidor-Reiss; Blachon et al., 2008); pUbq YFP-CNB and pUbq YFP-CNB$^{T4A-T9A-S82A}$ (Januschke et al., 2013); and UNC-GFP (Baker et al., 2004). Throughout the study, *Cnb* mutant refers to PBac{RB}Cnb^{e00267}/Df(3L)ED4284. This allelic combination causes the loss of interphase asters in larval neuroblasts as effectively as Cnb-RNAi driven from ubiquitous promoters. However, unlike RNAi-driven CNB depletion, this allelic combination does not have any significant effect on adult viability (Januschke et al., 2013). All crosses were performed at 25°C.

Fertility tests

Fertility tests were performed by scoring the offspring from each of 15 males individually mated to three w^{1118} females.

Immunocytochemistry

Testes from pupae were dissected in PBS and placed in a small drop of 5% glycerol in PBS on a glass slide, squashed under a small coverslip, and frozen in liquid nitrogen. After removal of the coverslip, the samples were immersed in methanol for 10 min at −20°C followed by 15 min in PBS and 1 h in PBS containing 0.1% BSA (PBS-BSA). Samples were then incubated with primary antibodies in a humid chamber either for 1 h at room temperature or overnight at 4°C, washed in PBS-BSA three times for 10 min, incubated for 1 h at room temperature with Alexa Fluor–conjugated secondary antibodies (Invitrogen), and then washed again as before. Immunostained preparations were mounted in small drops of Vectashield (Vector Laboratories). Images were taken with either an AxioImager Z1 microscope equipped with an AxioCam HR cooled charge-coupled camera using a 100× objective (ZEISS) or an SP8 confocal lens mounted on a DMIRBE2 microscope using an 63× 1.47 NA objective (Leica Microsystems). Acquired images were processed using ImageJ (1.48s; National Institutes of Health). Grayscale digital images were collected separately and then pseudocolored and merged using Photoshop (7.0; Adobe). Final figures were prepared using Illustrator (Adobe). First antibodies: rabbit anti–DSas-4 (from J. Gopalakrishnan; Gopalakrishnan et al., 2011), DM1a anti–α-TUB (1:500; T9026; Sigma-Aldrich), rabbit anti-Asl (1:500; Januschke et al., 2013), mouse antiacetylated Tub (1:500; T6793; Sigma-Aldrich), chicken anti-PLP (from A. Rodrigues-Martins; Rodrigues-Martins et al., 2007), and rabbit anti-CNB (1:500). Alexa Fluor conjugates were used at 1:1,000 dilution. DNA was stained with DAPI.

Production of anti-CNB antibody

A PCR fragment encoding amino acids 235–549 of CNB was subcloned into the pHAT vector (European Molecular Biology Laboratory). The resulting 6×His protein fusion protein was purified using TALON resin (Takara Bio Inc.) according to the manufacturer's instructions and was used to generate rabbit antibodies at Harlan (ENVIGO).

Fluorescence-based estimation of centriole length

As a proxy for centriole length, we measured the distance between the distal end of the YFP-ASL signal and the point at which both centrioles intersect on the internal part of the V shape. Because emitted light scatters over an area that is larger than the actual fluorescent particle, measurements based on fluorescent labels overestimate the actual particle's size. EM-based measurements provided much more precise data.

Phase-contrast microscopy

Phase-contrast microscopy of nonfixed testes was performed as previously described (Glover and González, 1993). In brief, testes were dissected and placed in a small drop of PBS on a siliconized slide, cut at about one third from its apical end with tungsten needles, covered with a coverslip, and gently squashed by removing the PBS with a small piece of blotting paper. We used a 40× dry phase-contrast objective. Images were acquired with an AxioCam MRm camera (ZEISS).

Transmission EM

Testes isolated from larvae and pupae were prefixed in 2.5% glutaraldehyde buffered in PBS overnight at 4°C. After prefixation, the material was carefully rinsed in PBS and postfixed in 1% osmium tetroxide in PBS for 2 h at 4°C. Samples were then washed in the same buffer, dehydrated in a graded series of ethanol, embedded in a mixture of epon-Araldite, and polymerized at 60°C for 48 h. 50–60-nm-thick sections were obtained with an Ultracut E ultramicrotome (Reichert) equipped with a diamond knife, mounted on copper grids, and stained with uranyl acetate and lead citrate. Images were taken with either a CM 10 transmission electron microscope (Philips) operating at an accelerating voltage of 80 kV or a Tecnai Spirit transmission electron microscope (FEI) operating at 100 kV equipped with a Morada charge-coupled device camera (Olympus).

Statistical analysis

We performed one-way ANOVA tests using Prism (GraphPad Software). Error bars represent SEM.

Online supplemental material

Fig. S1 shows EM sections showing that basal body–CLR complexes in *Cnb* mutant early spermatids retain the ultrastructural defects observed in early spermatocytes, immunofluorescence and phase-contrast microscopy documenting normal meiosis in *Cnb* mutant males, and immunofluorescence staining of CNB in WT spermatids. Fig. S2 shows ultrastructural details of a *Cnb* mutant axoneme that presents triplets with open sheaths as well as immunofluorescence showing scattered nuclei over the tails in *Cnb* mutant spermatids. Table S1 shows the number of C-tubules observed in 11 *Cnb* mutant basal bodies. Table S2 shows the mother and daughter basal body length in WT and *Cnb* mutant males.

Acknowledgments

We thank T. Avidor-Reiss, J. Gopalakrishnan, A. Rodrigues-Martins, and the Bloomington Drosophila Stock Center for providing

antibodies and fly lines, and G. Pollarolo for helpful discussions and suggestions.

Work in our laboratory is supported by Ministerio de Economía y Competitividad (MINECO; Government of Spain) grants BFU2015-66304-P and Redes de Excelencia BFU2014-52125-REDT-CellSYS as well as Generalitat de Catalunya grant SGR Agaur 2014-100. The Institute for Research in Biomedicine (IRB Barcelona) is the recipient of a Severo Ochoa Award of Excellence from MINECO. M. Gottardo is supported by a fellowship from the Alexander von Humboldt Foundation.

The authors declare no competing financial interests.

Author contributions: M. Gottardo, S. Llamazares, J. Reina, M.G. Riparbelli, G. Callaini, and C. Gonzalez conceived and designed the experiments and analyzed the data. J. Reina generated the antibodies. S. Llamazares and G. Callaini performed immunofluorescence microscopy. M. Gottardo, M.G. Riparbelli, and G. Callaini performed EM. C. Gonzalez wrote the manuscript.

Submitted: 6 January 2018
Revised: 16 April 2018
Accepted: 24 April 2018

References

Baker, J.D., S. Adhikarakunnathu, and M.J. Kernan. 2004. Mechanosensory-defective, male-sterile unc mutants identify a novel basal body protein required for ciliogenesis in Drosophila. *Development.* 131:3411–3422. https://doi.org/10.1242/dev.01229

Basiri, M.L., A. Ha, A. Chadha, N.M. Clark, A. Polyanovsky, B. Cook, and T. Avidor-Reiss. 2014. A migrating ciliary gate compartmentalizes the site of axoneme assembly in Drosophila spermatids. *Curr. Biol.* 24:2622–2631. https://doi.org/10.1016/j.cub.2014.09.047

Blachon, S., J. Gopalakrishnan, Y. Omori, A. Polyanovsky, A. Church, D. Nicastro, J. Malicki, and T. Avidor-Reiss. 2008. Drosophila asterless and vertebrate Cep152 Are orthologs essential for centriole duplication. *Genetics.* 180:2081–2094. https://doi.org/10.1534/genetics.108.095141

Blachon, S., X. Cai, K.A. Roberts, K. Yang, A. Polyanovsky, A. Church, and T. Avidor-Reiss. 2009. A proximal centriole-like structure is present in Drosophila spermatids and can serve as a model to study centriole duplication. *Genetics.* 182:133–144. https://doi.org/10.1534/genetics.109.101709

Carvalho-Santos, Z., P. Machado, I. Alvarez-Martins, S.M. Gouveia, S.C. Jana, P. Duarte, T. Amado, P. Branco, M.C. Freitas, S.T. Silva, et al. 2012. BLD10/CEP135 is a microtubule-associated protein that controls the formation of the flagellum central microtubule pair. *Dev. Cell.* 23:412–424. https://doi.org/10.1016/j.devcel.2012.06.001

Dutcher, S.K., and E.C. Trabuco. 1998. The UNI3 gene is required for assembly of basal bodies of Chlamydomonas and encodes delta-tubulin, a new member of the tubulin superfamily. *Mol. Biol. Cell.* 9:1293–1308. https://doi.org/10.1091/mbc.9.6.1293

Fritz-Niggli, H., and T. Suda. 1972. Bildung und Bedeutung der Zentriolen: Eine Studie und Neuinterpretation der Meiose von Drosophila [Formation and significance of centrioles: A study and new interpretation of the meiosis of Drosophila]. *Cytobiologie.* 5:12–41.

Fu, J., and D.M. Glover. 2012. Structured illumination of the interface between centriole and peri-centriolar material. *Open Biol.* 2:120104. https://doi.org/10.1098/rsob.120104

Galletta, B.J., R.X. Guillen, C.J. Fagerstrom, C.W. Brownlee, D.A. Lerit, T.L. Megraw, G.C. Rogers, and N.M. Rusan. 2014. Drosophila pericentrin requires interaction with calmodulin for its function at centrosomes and neuronal basal bodies but not at sperm basal bodies. *Mol. Biol. Cell.* 25:2682–2694. https://doi.org/10.1091/mbc.E13-10-0617

Garreau de Loubresse, N., F. Ruiz, J. Beisson, and C. Klotz. 2001. Role of delta-tubulin and the C-tubule in assembly of Paramecium basal bodies. *BMC Cell Biol.* 2:4. https://doi.org/10.1186/1471-2121-2-4

Glover, D.M., and C. González. 1993. Techniques for studying mitosis in Drosophila. *In* The Cell Cycle: a Practical Approach. R. Brookes, and P. Fantes, editors. IRL Press, Oxford, England, UK. 163–168.

González, C., J. Casal, and P. Ripoll. 1989. Relationship between chromosome content and nuclear diameter in early spermatids of Drosophila melanogaster. *Genet. Res.* 54:205–212. https://doi.org/10.1017/S0016672300028664

Gopalakrishnan, J., V. Mennella, S. Blachon, B. Zhai, A.H. Smith, T.L. Megraw, D. Nicastro, S.P. Gygi, D.A. Agard, and T. Avidor-Reiss. 2011. Sas-4 provides a scaffold for cytoplasmic complexes and tethers them in a centrosome. *Nat. Commun.* 2:359. https://doi.org/10.1038/ncomms1367

Gottardo, M., G. Callaini, and M.G. Riparbelli. 2013. The cilium-like region of the Drosophila spermatocyte: an emerging flagellum? *J. Cell Sci.* 126:5441–5452. https://doi.org/10.1242/jcs.136523

Gottardo, M., G. Pollarolo, S. Llamazares, J. Reina, M.G. Riparbelli, G. Callaini, and C. Gonzalez. 2015. Loss of Centrobin Enables Daughter Centrioles to Form Sensory Cilia in Drosophila. *Curr. Biol.* 25:2319–2324. https://doi.org/10.1016/j.cub.2015.07.038

Gudi, R., C. Zou, J. Li, and Q. Gao. 2011. Centrobin-tubulin interaction is required for centriole elongation and stability. *J. Cell Biol.* 193:711–725. https://doi.org/10.1083/jcb.201006135

Gudi, R., C. Zou, J. Dhar, Q. Gao, and C. Vasu. 2014. Centrobin-centrosomal protein 4.1-associated protein (CPAP) interaction promotes CPAP localization to the centrioles during centriole duplication. *J. Biol. Chem.* 289:15166–15178. https://doi.org/10.1074/jbc.M113.531152

Gudi, R., C.J. Haycraft, P.D. Bell, Z. Li, and C. Vasu. 2015. Centrobin-mediated regulation of the centrosomal protein 4.1-associated protein (CPAP) level limits centriole length during elongation stage. *J. Biol. Chem.* 290:6890–6902. https://doi.org/10.1074/jbc.M114.603423

Januschke, J., S. Llamazares, J. Reina, and C. Gonzalez. 2011. Drosophila neuroblasts retain the daughter centrosome. *Nat. Commun.* 2:243. https://doi.org/10.1038/ncomms1245

Januschke, J., J. Reina, S. Llamazares, T. Bertran, F. Rossi, J. Roig, and C. Gonzalez. 2013. Centrobin controls mother-daughter centriole asymmetry in Drosophila neuroblasts. *Nat. Cell Biol.* 15:241–248. https://doi.org/10.1038/ncb2671

Jeffery, J.M., A.J. Urquhart, V.N. Subramaniam, R.G. Parton, and K.K. Khanna. 2010. Centrobin regulates the assembly of functional mitotic spindles. *Oncogene.* 29:2649–2658. https://doi.org/10.1038/onc.2010.37

Jeffery, J.M., I. Grigoriev, I. Poser, A. van der Horst, N. Hamilton, N. Waterhouse, J. Bleier, V.N. Subramaniam, I.V. Maly, A. Akhmanova, and K.K. Khanna. 2013. Centrobin regulates centrosome function in interphase cells by limiting pericentriolar matrix recruitment. *Cell Cycle.* 12:899–906. https://doi.org/10.4161/cc.23879

Jeong, Y., J. Lee, K. Kim, J.C. Yoo, and K. Rhee. 2007. Characterization of NIP2/centrobin, a novel substrate of Nek2, and its potential role in microtubule stabilization. *J. Cell Sci.* 120:2106–2116. https://doi.org/10.1242/jcs.03458

Lerit, D.A., and N.M. Rusan. 2013. PLP inhibits the activity of interphase centrosomes to ensure their proper segregation in stem cells. *J. Cell Biol.* 202:1013–1022. https://doi.org/10.1083/jcb.201303141

Liška, F., C. Gosele, E. Popova, B. Chylíková, D. Křenová, V. Křen, M. Bader, L.L. Tres, N. Hubner, and A.L. Kierszenbaum. 2013. Overexpression of full-length centrobin rescues limb malformation but not male fertility of the hypodactylous (hd) rats. *PLoS One.* 8:e60859. https://doi.org/10.1371/journal.pone.0060859

Ma, L., and A.P. Jarman. 2011. Dilatory is a Drosophila protein related to AZI1 (CEP131) that is located at the ciliary base and required for cilium formation. *J. Cell Sci.* 124:2622–2630. https://doi.org/10.1242/jcs.084798

Ogungbenro, Y.A., T.C. Tena, D. Gaboriau, P. Lalor, P. Dockery, M. Philipp, and C.G. Morrison. 2018. Centrobin controls primary ciliogenesis in vertebrates. *J. Cell Biol.* 217:1205–1215. https://doi.org/10.1083/jcb.201706095

Rebollo, E., P. Sampaio, J. Januschke, S. Llamazares, H. Varmark, and C. González. 2007. Functionally unequal centrosomes drive spindle orientation in asymmetrically dividing Drosophila neural stem cells. *Dev. Cell.* 12:467–474. https://doi.org/10.1016/j.devcel.2007.01.021

Riparbelli, M.G., and G. Callaini. 2011. Male gametogenesis without centrioles. *Dev. Biol.* 349:427–439. https://doi.org/10.1016/j.ydbio.2010.10.021

Riparbelli, M.G., G. Callaini, and T.L. Megraw. 2012. Assembly and persistence of primary cilia in dividing Drosophila spermatocytes. *Dev. Cell.* 23:425–432. https://doi.org/10.1016/j.devcel.2012.05.024

Riparbelli, M.G., O.A. Cabrera, G. Callaini, and T.L. Megraw. 2013. Unique properties of Drosophila spermatocyte primary cilia. *Biol. Open.* 2:1137–1147. https://doi.org/10.1242/bio.20135355

Rodrigues-Martins, A., M. Bettencourt-Dias, M. Riparbelli, C. Ferreira, I. Ferreira, G. Callaini, and D.M. Glover. 2007. DSAS-6 organizes a tube-like centriole precursor, and its absence suggests modularity in centriole

assembly. *Curr. Biol.* 17:1465–1472. https://doi.org/10.1016/j.cub.2007.07.034

Shin, W., N.K. Yu, B.K. Kaang, and K. Rhee. 2015. The microtubule nucleation activity of centrobin in both the centrosome and cytoplasm. *Cell Cycle.* 14:1925–1931. https://doi.org/10.1080/15384101.2015.1041683

Singh, P., A. Ramdas Nair, and C. Cabernard. 2014. The centriolar protein Bld10/Cep135 is required to establish centrosome asymmetry in Drosophila neuroblasts. *Curr. Biol.* 24:1548–1555. https://doi.org/10.1016/j.cub.2014.05.050

Tates, A.D. 1971. Cytodifferentiation during spermatogenesis in Drosophila melanogaster: an electron microscope study. Proefschrift, Rijksuniversiteit te Leiden, Leiden, The Netherlands. 162.

Vieillard, J., M. Paschaki, J.L. Duteyrat, C. Augière, E. Cortier, J.A. Lapart, J. Thomas, and B. Durand. 2016. Transition zone assembly and its contribution to axoneme formation in Drosophila male germ cells. *J. Cell Biol.* 214:875–889. https://doi.org/10.1083/jcb.201603086

Zheng, X., A. Ramani, K. Soni, M. Gottardo, S. Zheng, L. Ming Gooi, W. Li, S. Feng, A. Mariappan, A. Wason, et al. 2016. Molecular basis for CPAP-tubulin interaction in controlling centriolar and ciliary length. *Nat. Commun.* 7:11874. https://doi.org/10.1038/ncomms11874

Zou, C., J. Li, Y. Bai, W.T. Gunning, D.E. Wazer, V. Band, and Q. Gao. 2005. Centrobin: a novel daughter centriole-associated protein that is required for centriole duplication. *J. Cell Biol.* 171:437–445. https://doi.org/10.1083/jcb.200506185